Physics Letters B 294 (1992) 263–268
North-Holland

PHYSICS LETTERS B

Screening in the lattice Schwinger model

Hermann Dilger

Deutsches Elektronen-Synchrotron DESY, Notkestraße 85, W-2000 Hamburg 52, FRG

Received 13 August 1992

We calculate the potential between heavy fermions in the lattice Schwinger model in the euclidean formalism with staggered fermions by an unquenched strong coupling expansion and Monte Carlo simulations. The results are compared with the corresponding continuum expressions including finite size corrections.

1. Introduction

Up to now attempts to show the screening of the colour charge in QCD have had only limited success [1]. It appears difficult to see the influence of the fermion determinant in Monte Carlo (MC) simulations and to distinguish between screening and finite volume effects. We address these questions within the Schwinger model (SM) on a euclidean lattice with massless staggered fermions, because the SM is exactly solvable and shows the screening property too [2]. For the comparison with our staggered fermion calculations we refer to the solution of the "geometric" SM on the torus T_2 [3,4], which is essentially the SM with two fermion species. The advantage of taking staggered fermions and comparing with the "geometric" continuum SM is the well-defined connection between lattice and continuum [5], while totally breaking the chiral symmetry on the lattice is avoided [6].

In this letter we calculate gauge field observables with MC simulations and using an unquenched strong coupling expansion (SCE) up to order $N = 3$ for a fixed volume. In particular, we show how the lattice reproduces the screening behaviour. Finite volume effects and topological questions, as far as they concern gauge field variables, can be treated explicitly.

Screening within the SM has already been investigated in the hamiltonian formalism by Bender, Rothe and Rothe [7] and Potvin [8]. Other authors use the SM in order to test MC algorithms [9,10]. For that it might be useful to have control over the effects of finite volume and finite lattice spacing.

The paper is organized as follows: In section 2 we present the pure gauge results, in section 3 we perform the SCE for the unquenched theory, whereas section 4 gives the results of our MC simulations. In section 5 we conclude and give an outlook to further work to be done.

2. Pure gauge theory

2.1. Lattice Schwinger model

The Wilson action of the lattice Schwinger model is given by

$$S_g = \tfrac{1}{2}\overline{\beta}\sum_x (2 - P_x - P_x^{-1}) ,$$

$$P_x = U_{[x,1]}\, U_{[x+e_1,2]}\, U^{-1}_{[x+e_2,1]}\, U^{-1}_{[x,2]} . \qquad (1)$$

Quantities in units of the lattice spacing a, as $\overline{\beta}$, are marked by a bar.

In order to calculate the expectation values of Wilson loops $W[U]$ a strong coupling expansion, combined with a duality transformation [11] can be performed. For an infinitely large lattice this yields immediately

$$\langle W\rangle_g \equiv \int \mathcal{D}[U]\, W[U] \exp(-S_g[U]) = \widetilde{I}_1(\overline{\beta})^{\overline{A}} ,$$

$$\widetilde{I}_k(\overline{\beta}) = I_k(\overline{\beta})/I_0(\overline{\beta}) . \qquad (2)$$

Here $\overline{A}, \overline{V}$ are the area of W and the volume of the lattice in lattice units and I_k denote the modified Bessel functions of order k. With the asymptotic expansion of $\widetilde{I}_k$ up to second order (see e.g. ref. [12]) we find on a finite lattice with periodic boundary conditions

$$\langle W\rangle_g = \exp\left[-\frac{A}{2\beta}\left(1+\frac{a^2}{2\beta}\right)\right]\frac{\Theta_3((A/V)\tau \mid \tau)}{\Theta_3(0 \mid \tau)} + O(a^4),$$

$$\tau = \frac{iV}{2\pi\beta}\left(1+\frac{a^2}{2\beta}\right). \tag{3}$$

Here the values A, V, β are fixed in physical units, while $\overline{\beta} = \beta/a^2$ etc. For our definition of Jacobi's function $\Theta_3(z \mid \tau)$ see ref. [13].

We want to compare this result with the non-compact formulation of the gauge field variables with a simple quadratic lattice action. In this case we get

$$\langle W\rangle_g = \exp\left[-\frac{A}{2\beta}\left(1-\frac{A}{V}\right)\right]. \tag{4}$$

The last two equations show the well-known fact that the scaling behaviour of the lattice SM is trivial, i.e., in the limit $a \to 0$ we get scaling by $\overline{\beta} = 1/e^2a^2$, e is the physical coupling constant.

2.2. Continuum SM

For the corresponding calculations in the continuum SM on the torus $\mathcal{T}_2$ we follow the definitions given in ref. [3]. There, a general gauge potential in Lorentz gauge is written as

$$A_\mu = t_\mu + \epsilon_{\mu\nu}\partial_\nu b(x) - \tfrac{1}{2}c_k\epsilon_{\mu\nu}x_\nu,$$

$$c_k = \frac{2\pi k}{eV}, \tag{5}$$

$k \in \mathbb{Z}$ gives the topological sector of A_μ, $V = L \times T$ is the volume of $\mathcal{T}_2$. If we restrict A_μ to the topologically trivial sector, the expectation value of a Wilson loop W of area A becomes

$$\langle W\rangle^{(0)}_{g,C} = \exp\left[-\tfrac{1}{2}e^2A\left(1-\frac{A}{V}\right)\right]. \tag{6}$$

This is exactly the result of the non-compact lattice calculation eq. (4) with $\beta = 1/e^2$. In fact, it is easy to see that the non-compact lattice formulation suppresses the topologically non-trivial gauge configurations $[A_{nt}]$ with $S_g^{\text{non-compact}}[A_{nt}] \sim 1/a^2$ in the continuum limit.

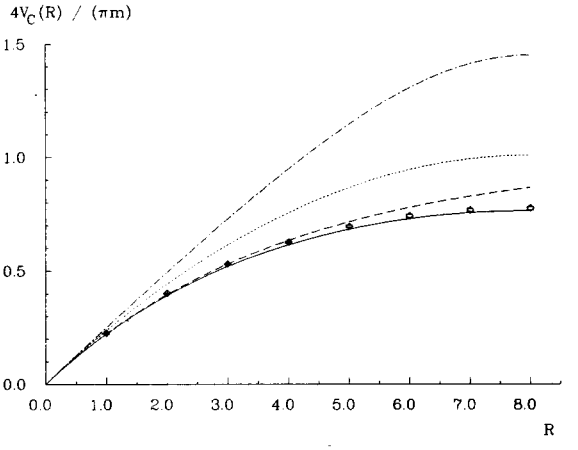

Fig. 1. Continuum potential: unquenched (full line), unquenched with infinite volume approximation (dashed), quenched non-compact (dotted) and quenched compact (dash-dotted). The squares show MC measurements for $\overline{\beta} = 10$.

The inclusion of the topologically non-trivial sectors leads to

$$\langle W\rangle_{g,C} = \exp(-\tfrac{1}{2}e^2A)\frac{\Theta_3((A/V)\tau_C \mid \tau_C)}{\Theta_3(0 \mid \tau_C)},$$

$$\tau_C = \frac{ie^2V}{2\pi}, \tag{7}$$

which agrees with the result of the compact lattice formulation in the limit $a \to 0$.

In fig. 1 we give the potential between two heavy fermions for $L = 16$, $T = 6$, $\beta = 10$. It is extracted from the expectation values in eqs. (6), (7) of an $R \times T$ Wilson loop, i.e., two opposite Polyakov loops $\mathrm{PL}(R)$ at distance R

$$V_C(R) = \frac{-1}{T}\ln\langle \mathrm{PL}(R)\rangle_{g,C}. \tag{8}$$

3. SCE with dynamical fermions

We denote the action of massless staggered fermions by

$$S_f = \frac{1}{2a}\sum_{x,\mu}\rho_\mu(x)[\overline{\chi}(x)U_{[x,\mu]}\chi(x+e_\mu) - \text{h.c.}]$$

$$\equiv \frac{1}{2a}\overline{\chi}Q[U]\chi. \tag{9}$$

After integration of the fermionic variables we get the expectation value of a gauge field observable $\Omega[U]$,

$$\langle\Omega\rangle = \frac{Y_\Omega}{Z} \equiv \frac{\langle\Omega[U]\det Q[U]\rangle_g}{\langle\det Q[U]\rangle_g} . \tag{10}$$

The fermion determinant is usually treated with Wilson fermions using the hopping parameter expansion [14]. For the staggered fermion determinant such an expansion is not known yet. Instead, one proceeds with its evaluation by the Cramer rule [15]

$$\det Q[U] = \sum_G \omega_G[U] ,$$

$$\omega_G[U] = (-1)^n \prod_{[x,\mu]\in G} \mathrm{sign}(\mu)\rho_\mu(x)U_{[x,\mu]} . \tag{11}$$

Here G is a general graph consisting of n oriented loops, which touches every lattice point exactly once. The smallest loop, consisting of two opposite links, is called a dimer. It has no orientation and the weight $\omega = 1$. In the infinite volume limit the gauge field integration in eq. (10) gives a factor $\widetilde{I}_1(\overline{\beta})^A$ to every graph G surrounding $\overline{A}$ plaquettes once [#1]. So $\widetilde{I}_1(\overline{\beta}) \equiv \gamma$ will serve as the expansion parameter of a strong coupling expansion. We neglect the finite volume corrections because they are of order $\gamma^{(\overline{V}-\overline{A})}$.

In the further evaluation in the next two subsections all quantities are understood in lattice units, but for simplicity of notation we drop the bars.

3.1. Zero order strong coupling approximation

In zero order strong coupling approximation a U(n) theory with staggered fermions is equivalent to a dense dimer gas [15], since dimers are the only loops with trivial gauge factor. We have

$$Z^0 = \sum_D 1, \quad Y^0_\Omega = \mathrm{sign}(\Omega)\sum_{D_\Omega} 1 , \tag{12}$$

where D is a general combination of dimers covering all lattice points but having no points in common, for D_Ω the dimers are not allowed to touch Ω either. In the lattice SM either $\mathrm{sign}(\Omega)$ is positive or Y^0_Ω vanishes (see e.g. ref. [16]). For the further calculation we use the representation of the sums in eq. (12) as integrals over Grassmann variables given by Samuel [17]. The effect of the double periodic boundary conditions on T_2 are treated with methods described in ref. [18]. The result is

$$Z^0 = \tfrac{1}{2}(Z^{--} + Z^{-+} + Z^{+-}),$$

$$Y^0_\Omega = \tfrac{1}{2}(Y^{--}_\Omega + Y^{-+}_\Omega + Y^{+-}_\Omega - Y^{++}_\Omega),$$

$$Z^{\epsilon_1\epsilon_2} = \int \mathcal{D}[\overline{\phi},\phi]\exp(-\overline{\phi}Q_f^{\epsilon_1\epsilon_2}\phi) ,$$

$$Y^{\epsilon_1\epsilon_2}_\Omega = \left|\int \mathcal{D}[\overline{\phi},\phi]\exp(-\overline{\phi}Q_f^{\epsilon_1\epsilon_2}\phi)\prod_{x\in\Omega}\widetilde{\phi}(x)\right| . \tag{13}$$

Here $\overline{\phi}$ lives on the even, ϕ on the odd sites of the lattice, $Q_f^{\epsilon_1\epsilon_2}$ is the fermion matrix of eq. (9) restricted accordingly without gauge fields, $\epsilon_1(\epsilon_2) = \pm 1$ denote periodic and antiperiodic boundary conditions in space (time) direction, respectively. Furthermore $\widetilde{\phi}(x) = \overline{\phi}(x)$ $(\phi(x))$ for x even (odd). Doing again the Grassmann integrals we get

$$Z^{\epsilon_1\epsilon_2} = \prod_{\{p\}^{\epsilon_1\epsilon_2}} \left(4\sum_{\mu=1,2}\sin^2 p_\mu\right) . \tag{14}$$

With $L_1 \equiv L$, $L_2 \equiv T$ the momenta p in $\{p\}^{\epsilon_1\epsilon_2}$ are given by

$$p_\mu = \frac{2\pi}{L_\mu}(n_\mu + \alpha_{\epsilon_\mu}) , \quad n_\mu \in [-\tfrac{1}{4}L_\mu, \tfrac{1}{4}L_\mu)\cap\mathbb{Z} ,$$

$$\alpha_+ = 0, \quad \alpha_- = \tfrac{1}{2} . \tag{15}$$

The $Y^{\epsilon_1\epsilon_2}_\Omega$ can be calculated by $Y^{\epsilon_1\epsilon_2}_\Omega = Z^{\epsilon_1\epsilon_2} y^{\epsilon_1\epsilon_2}_\Omega$, $y^{\epsilon_1\epsilon_2}_\Omega$ is the usual n-point function of the free fermion action in eq. (13). For that a sensible limit has to be taken for the zero mode appearing with $\epsilon_1\epsilon_2 = + +$. It causes Z^{++} to be 0, while in general $Y^{++}_\Omega \neq 0$. This gives in principle the zeroth order strong coupling expectation value of all observables $\Omega[U]$. However, in practice, e.g., for Polyakov loops the sum over permutations in the n-point functions y_Ω is not very practicable.

In two dimensions it is possible to calculate the Y^0_Ω for $\Omega = \mathrm{PL}(R)$, i.e., two opposite Polyakov loops at distance R, as

$$Y^0_{\mathrm{PL}(R)} = Z_{\mathrm{PL}}(R)Z_{\mathrm{PL}}(L-R), \tag{16}$$

where $Z_{\mathrm{PL}}(R)$ is the dimer gas partition function on a $R\times T$ lattice with boundary conditions simulating the presence of a Polyakov loop. We obtain

[#1] A plaquette surrounded k times gives rise to a factor $\widetilde{I}_k(\overline{\beta})$, but this does not occur up to the regarded orders.

$$Z_{\mathrm{PL}}(R) = \prod_{p_1,p_2}\Big(4\sum_{\mu=1,2}\sin^2 p_\mu\Big) \quad \text{for } R \text{ odd},$$
$$= \prod_{p_2}|2\sin p_2|\prod_{p_1}\Big(4\sum_{\mu=1,2}\sin^2 p_\mu\Big) \quad \text{for } R \text{ even}, \tag{17}$$

where p_1, p_2 take the values $p_1 = \pi/2R, 3\pi/2R, \ldots, (R-2)\pi/2R$, for R odd, $p_1 = \pi/R, 2\pi/R, \ldots, (\frac{1}{2}R-1)\pi/R$, for R even, $p_2 = 2\pi(n_2+\frac{1}{2})/T$, $n_2 \in [-\frac{1}{4}T, \frac{1}{4}T) \cap \mathbb{Z}$.

3.2. SCE of $\langle\Omega\rangle$ up to the Nth order

For a SCE of $\langle\Omega\rangle$ up to the Nth order we define $\widetilde{\mathrm{G}}$ to be a graph G where all dimers have been omitted and $\mathrm{ord}(\widetilde{\mathrm{G}})$ to be the power of γ with which the corresponding Wilson loops would be weighted after gauge integration in pure gauge theory. So we have to do the sums

$$Z^N = Z^0\Big(1 + \sum_{n=1}^{N}\gamma^n \sum_{\widetilde{\mathrm{G}},\mathrm{ord}(\widetilde{\mathrm{G}})=n} x(\widetilde{\mathrm{G}})\Big), \tag{18}$$

$x(\widetilde{\mathrm{G}}) \equiv Y^0_{\widetilde{\mathrm{G}}}/Z^0$ is the zero order expectaion value of $\widetilde{\mathrm{G}}$, given by eq. (13),

$$Y^N_\Omega = Y^0_\Omega\Big(1 + \sum_{n=1}^{N}\gamma^n \sum_{\widetilde{\mathrm{G}},\mathrm{ord}(\widetilde{\mathrm{G}}\cup\Omega)=n} x_\Omega(\widetilde{\mathrm{G}})\Big). \tag{19}$$

For $\Omega = \mathrm{PL}(R)$, $x_\Omega(\widetilde{\mathrm{G}}) \equiv Y^0_{\widetilde{\mathrm{G}}\cup\Omega}/Y^0_\Omega$ can be computed as the n-point function under the Polyakov loop boundary conditions mentioned above.

We define the Nth order SC approximation of the potential $\overline{V}(\overline{R})$ in two ways: $\overline{V}^N(\overline{R})$ and $\widetilde{V}^N(\overline{R})$. For $\overline{V}^N(\overline{R})$ the expansion of $\overline{V}(\overline{R})$, defined as in eq. (8), terminates with the Nth power of γ, whereas for $\widetilde{V}^N(\overline{R}) = -\ln W^N(\overline{R})/\overline{T}$ the expansion of $W(\overline{R}) = \langle\mathrm{PL}(\overline{R})\rangle$ terminates with the Nth power of γ.

For a comparison with Monte Carlo data we have evaluated these potentials for a 16×6 lattice up to order $N = 3$, see figs. 2,3 for $\widetilde{V}^N$. With the "convergence criterion" $|\overline{V}^3(\overline{R}) - \overline{V}^2(\overline{R})| < |\overline{V}^2(\overline{R}) - \overline{V}^1(\overline{R})|$ for all R we found "convergence" up to $\overline{\beta} = 0.6$. For $\overline{T} = 6$ it appears that the convergence is faster for $\widetilde{V}^N$, in particular $\widetilde{V}^N$ decreases uniformly with $N = 0, 1, 2, 3$, whereas the corrections in V^N change their sign with each N.

3.3. Continuum SM

For the continuum SM on $\mathcal{T}_2$ in the "geometric" formulation the potential given by the Polyakov loop correlation is calculated as [4]

$$V_{\mathrm{C}}(R) = \tfrac{1}{4}\pi m[1 - \exp(-mR)] - \frac{\pi m(\cosh mR - 1)}{2[\exp(mL) - 1]},$$
$$m^2 = \frac{2e^2}{\pi}. \tag{20}$$

The finite volume correction is only given by L, i.e., $V_{\mathrm{C}}(R)$ does not depend on T. In the limit $mL \to \infty$ the second term in eq. (20) vanishes and the well-known screening potential remains, see fig. 1.

For a potential $\overline{V}(\overline{R})$ on a lattice with the same size as $\mathcal{T}_2$ in physical units we expect for $a \to 0$ scaling as in the pure gauge theory with $\overline{\beta} = \beta/a^2$, $\beta = 1/e^2$, therefore for sufficiently small a

$$m^{-1}V_{\mathrm{C}}(R)|_\beta = \overline{m}^{-1}\overline{V}(\overline{R})|_{\overline{\beta}}, \quad \overline{m}^2 = \frac{2}{\pi\overline{\beta}}. \tag{21}$$

For gauge field observables, i.e., in our case the lattice potential $\overline{V}(\overline{R})$, no difference is expected between non-compact and compact lattice formulation in the scaling region, because $\det Q[U] \simeq 0$ for topologically non-trivial sectors. Therefore the influence of dynamical fermions on the potential is bigger in the compact case due to the suppression of these sectors by the fermion determinant, as can be seen in fig. 1.

4. Monte Carlo simulations

For the generation of gauge field configurations we used the hybrid Monte Carlo algorithm with pseudo-fermions [19]. As a check we did quenched simulations on a 10×10 lattice reproducing the results of section 2. With the trajectory length $\tau = 1$ we had to give the system hits changing the topological charge Q_{top} [20] (cf. ref. [9]). The unquenched potential defined as in eq. (8), was measured on a 16×6 lattice for various values of $\overline{\beta}$. The small extension in time direction $\overline{T} = 6$ was necessary to see clear signals for

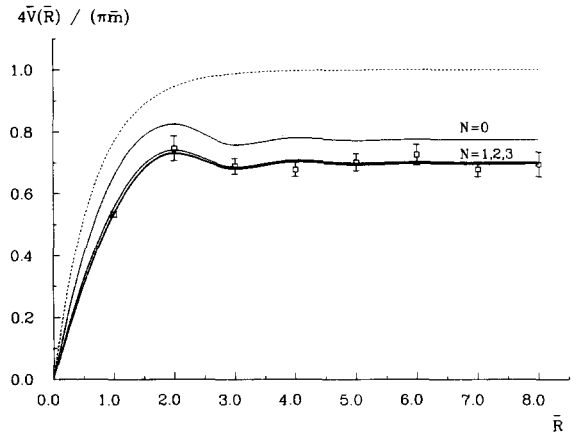

Fig. 2. Potential in the strong coupling region $\overline{\beta} = 0.3$: MC measurements, SCE up to order N, $\widetilde{V}^N$ (full lines, interpolated with a spline algorithm) and potential with assumed scaling eq. (21) (dotted line).

$\langle \mathrm{PL}(\overline{R}) \rangle$, in particular in the strong coupling region. However, this is no shortcoming at least in the scaling region, because there we expect no dependence on T as in the continuum equation (20). The estimation of autocorrelation times t_a was given by a jackknife procedure and checked by putting the data into a few blocks.

For $\overline{\beta} = 10$, after equilibration we generated 10 000 configurations each separated by five trajectories. All measured observables but Q_{top} showed correlation times $t_a \simeq 5$, for Q_{top} we found $t_a \simeq 50$. Using the scaling formula eq. (21) the Monte Carlo data for the potential are in agreement with the continuum result eq. (20) within the very small error bars, see fig. 1.

For $\overline{\beta} = 0.3$ fluctuations of the expectation values $\langle \mathrm{PL}(\overline{R}) \rangle$ exceeding the range of error bars could be seen up to a time of 20 000 trajectories. Therefore we started our measurement after 40 000 trajectories. Then autocorrelation times $t_a \simeq 3$ were found for all evaluated observables, so we took 30 000 configurations separated by two trajectories. The resulting potential $\overline{V}(\overline{R})$ matches the SCE, which converges rapidly in this region of $\overline{\beta}$, see fig. 2.

Finally we compare the strong coupling and scaling behaviour. At strong coupling $\overline{V}(\overline{R})$ is given by the SCE, thus it is constant with $\overline{\beta}$ in leading order, or – when next to leading orders come into play –

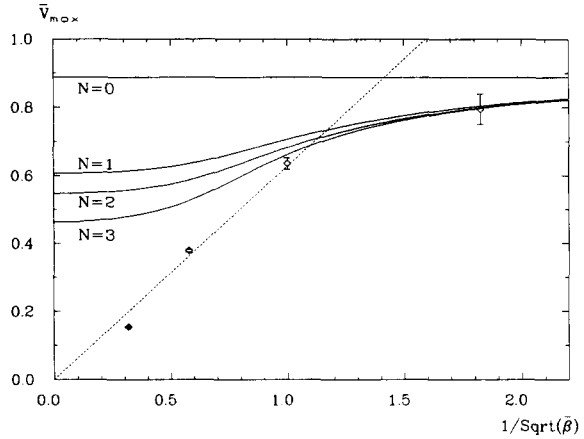

Fig. 3. $\overline{V}_{\mathrm{max}}$ versus $\overline{\beta}$: MC measurements, SCE up to order N, $\widetilde{V}^N$ (full lines) and scaling line without finite volume corrections (dotted line). The latter explain the deviation of the $\overline{\beta} = 10$ measurement, see fig. 1.

decreasing slowly as $\overline{\beta}$ increases. It appears that the first order remains important for relatively small $\overline{\beta}$. As a begins to resolve the screening length $R_{\mathrm{S}} = 1/m$ (usually [21] one requires $2a <$ typical length scale, i.e., $\overline{\beta} > 2.5$ in our case), we expect a transition to the scaling behaviour. Fig. 3 shows this for $\overline{V}_{\mathrm{max}} = \overline{V}(\frac{1}{2}\overline{L})$. As long as $\frac{1}{2}\overline{L} \gg \overline{R}_{\mathrm{S}}$ we should find $\overline{V}_{\mathrm{max}} \sim \overline{\beta}^{-1/2}$ in the scaling region. This is confirmed by the Monte Carlo data.

The $\overline{\beta} = 1.0$ measurement is surprisingly close to the scaling straight line. The reason must be a cancellation of $\mathrm{O}(a^2)$ effects (see the deviation of the point at $\overline{\beta} = 3.0$ from the scaling line) with higher order effects. On the other hand, the third order SCE at $\overline{\beta} = 1.0$ matches quite well with the MC data. However, here it is crucial to take the expansion given with $\widetilde{V}^N(\overline{R})$ rather than $\overline{V}^N(\overline{R})$, which converges better for small $\overline{T}$. Thus, although the region of seen convergence of the SCE: $\overline{\beta} < 0.6$ (see section 3) and the scaling region: $\overline{\beta} > 2.5$ are apart from each other, $\overline{\beta} = 1.0$ appears to be a good value for rough estimations on the lattice via SCE as well as MC simulations. The same could be seen for $\overline{V}(\overline{R})$ with different values of $\overline{R}$.

5. Conclusion

In the lattice SM with staggered fermions we did a

SCE up to third order for a fixed lattice size. It was compared with MC data and corresponding expressions in the continuum "geometric" SM, which explicitly include finite volume dependence.

The potential in the SCE shows the screening property (fig. 2) – if we assume values of $\overline{\beta}$ near the scaling border with a qualitatively correct value in the screening plateau (see fig. 3).

On the other hand, a comparison of the MC data with the continuum potential gives control over the effects of finite lattice spacing a as well as finite volume in the scaling region. For $\overline{\beta} = 10$ the finite a effects are already small. In order to see this, it is crucial to know the finite volume correction in the continuum, since it dominates the finite a effects here (see fig. 1). A comparison with the continuum expressions in pure gauge theory also shows how screening has to be distinguished from the strong finite volume corrections in the pure gauge theory and from the mere suppression of the topologically non-trivial field configurations. We could see explicitly how this suppression occurs when taking the non-compact instead of the compact lattice formulation in pure gauge theory.

It may be useful to treat the SM mass spectrum with similar methods in order to investigate the validity of the SCE for spectra and the influence of the quenched approximation thereby. It has to be remarked that for non-vanishing fermion mass and for dimensions $d > 2$ there are approximate results [17], which could be used instead of the exact formula eq. (13).

Moreover, the properties of the SCE should be investigated in more detail. In particular, we would like to know more about its large volume behaviour and the nature of the oscillations within the potential in the strong coupling region (see fig. 2).

Acknowledgement

I am much indebted to H. Joos for encouraging discussions and useful hints and to G. Schierholz for making a hybrid Monte Carlo computer program available to me. Furthermore I would like to thank M. Marcu for helpful hints on the literature.

References

[1] H. Joos and I. Montvay, Nucl. Phys. B 225 (1983) 565;
M. Campostrini et al., Phys. Lett. B 193 (1987) 78;
M. Fukugita et al., Phys. Lett. B 191 (1987) 164;
K.D. Born et al., Phys. Rev. D 40 (1990) 1653;
R. Gupta et al., Phys. Rev. D 44 (1991) 3272;
MT_c Collab., K.D. Born et al., The interquark potential: A QCD lattice analysis, in preparation.
[2] J. Schwinger, Phys. Rev. 128 (1962) 2425;
J. Lowenstein and A. Swieca, Ann. Phys. (NY) 68 (1971) 172.
[3] H. Joos, Nucl. Phys. B (Proc. Suppl.) 17 (1990) 704; Helv. Phys. Acta 63 (1990) 670.
[4] S.I. Azakov and H. Joos, The Schwinger model on the torus II, in preparation.
[5] P. Becher and H. Joos, Z. Phys. C 15 (1982) 343.
[6] H. Kluberg-Stern et al., Nucl. Phys. B 190 (1981) 504.
[7] I. Bender, H.J. Rothe and K.D. Rothe, Nucl. Phys. B 251 (1985) 745.
[8] J. Potvin, Phys. Rev. D 32 (1985) 2070.
[9] S. Gupta, Phys. Lett. B 278 (1992) 317.
[10] R. Ben-Av et al., Phys. Lett. B 253 (1991) 185; Bonn preprint BONN-HE-90-15.
[11] J.M. Drouffe and J.B. Zuber, J. Phys. Rep. 102 (1987) 1.
[12] I.S. Gradshteyn and I.M. Ryzhik, Table of integrals, series and products (San Diego, 1965).
[13] W. Magnus, F. Oberhettinger and R.P. Soni, Special functions of mathematical physics (Berlin, 1966).
[14] I. Montvay, Rev. Mod. Phys. 59 (1987) 263, and references therein.
[15] P. Rossi and U. Wolff, Nucl. Phys. B 284 (1984) 105.
[16] I. Montvay, Desy preprint DESY-89-051; Proc. Cargèse School (1989) p. 87.
[17] S. Samuel, J. Math. Phys. 21 (1980) 2806, 2815, 2820.
[18] B.M. McCoy and T.T. Wu, The two-dimensional Ising model (Cambridge, 1973) pp. 61–67.
[19] S. Duane et al., Phys. Lett. B 195 (1987) 216.
[20] J. Smit and J.C. Vink, Nucl. Phys. B 303 (1988) 36.
[21] M. Luescher and P. Weisz, Nucl. Phys. B 290 (1987) 25.